REVISTAMATÉRIA V.29 N.2
ISSN 1517-7076 articles e20230370, 2024

Influence of microstructure on the hardness and electrical conductivity of CuCrZr alloy submitted to ECAP followed by aging and rotary swaging

Talita Gama de Sousa[1], Wellington Mattos Pires[1], Renato Batista da Cruz[1], Luiz Paulo Brandão[1]

[1]Instituto Militar de Engenharia, Programa de Pós-Graduação em Ciência e Engenharia de Materiais. Praça General Tibúrcio, 80, 22290-270, Rio de Janeiro, RJ, Brasil.

e-mail: talitagama@ime.eb.br, wellington.mattos_pires@outlook.com, renato.materiais9@gmail.com, brandao@ime.eb.br

ABSTRACT

Grain boundaries are fundamental in the mechanical behavior of ultrafine grain materials, especially coincidence site lattice grain boundaries (CSL-GB). This research aims to identify the influence of CSL-GB on the hardness and electrical conductivity of a CuCrZr alloy subjected to rotary swaging after having undergone severe plastic deformation via equal channel angular pressing and aging. Vickers hardness was evaluated, and electrical conductivity was measured using the 4-point technique. The average grain size and CSL-GB distribution were identified using backscattered electron diffraction. Dislocation density was measured via X-ray diffraction. At the end of the swaging processing of CuCrZr alloy with preexistent ultrafine grains, the dislocation density ceases to be the significant influencer parameter on the modification of properties, and the grain boundaries pass to be more impacting. The reduction of CSL-GB and the concomitant increase in high-angle grain boundaries can decrease hardness and electrical conductivity.

Keywords: CuCrZr; Electrical conductivity; ECAP; EBSD; CSL grain boundaries.

1. INTRODUCTION

Technological advancement increasingly demands the development of high-performance materials, such as those combining high mechanical and electrical properties. The great challenge to obtain materials with this combination of properties is to strengthen suitable conductive materials, which are generally soft, through thermomechanical treatments without decreasing their electrical conductivity [1, 2].

Copper and copper base alloys are excellent options to achieve this properties combination; some copper base alloys can be highlighted: Cu-Mg, Cu-Cr, Al-Cu, Cu-Ag e Cu-Cr-Zr [3–7]. Some researchers [1, 8, 9] have shown that an excellent alternative to increase the strength of these alloys would be to subject them to a process of grain refinement by severe plastic deformation (SPD) [2] associated with an aging treatment. PURCEK *et al*. [1] obtained good properties combination in a CuCrZr alloy associating grain refinement by high-pressure torsion and aging. Recent studies [8, 9], mainly related to the ITER (International Thermonuclear Experimental Reactor) [10], have shown that subjecting a commercial CuCrZr alloy to the equal-channel angular pressing (ECAP) process followed by aging provided high hardness values without substantially impairing electrical conductivity in relation to pure Cu. Other studies combined ECAP with different processing steps and also obtained the maximization of the mechanical properties of the CuCrZr alloy [11].

SPD techniques are characterized by grain refinement, whose size reaches less than one μm [2, 12, 13]. Under deformation, the material microstructure passes through refinement until it reaches a steady state of ultrafine grains (UFG) [13]. These UFGs have a high density of grain boundaries (GBs), which can significantly define the material properties [14–17].

It is known that GBs have a fundamental role in the mechanical behavior of UFG materials [18, 19]. Depending on the deformation processing, there will be several types of grain boundaries, such as high angle, low angle, random, in equilibrium, and non-equilibrium grain boundaries [18, 20]. Therefore, controlling the grain size and evolution of the GBs' structures to manage physical properties in SPD processing is essential. As mentioned before, different grain boundaries can be formed in UFG materials [21, 22]. The ECAP technique creates low-angle grain boundaries (LAGB) under low deformation levels. As the deformation increases, the grains are progressively transformed into high-angle grain boundaries (HAGB) [12].

Corresponding Author: Talita Gama de Sousa Received on 21/12/2023 Accepted on 01/04/2024

DOI: https://doi.org/10.1590/1517-7076-RMAT-2023-0370

GBs can be geometrically classified according to the axis and angle of misorientation with some specific combinations [23]. Boundaries that show particular orientations (in which a significant fraction of lattice points are common to both grains) are called coincidence site lattice grain boundaries (CSL-GBs) [2]. The reciprocal of common point numbers in the lattice between two adjacent grains is represented by ∑. A well-known CSL-GB is the twin boundary defined by Σ3(<111> 60).

CSL-GBs with "low-∑" are known to have less energy [24], less susceptibility to solute segregation [25], outstanding resistance to slip [21], and excellent corrosion resistance [22]. Several researchers have shown that low-∑ CSL-GB, especially the twin boundaries, are less electrically active [15, 16, 26], or in other words, have low electrical resistivity [27, 28]. In addition, their pronounced presence can improve mechanical strength [29].

Some authors [30–33] have already reported the presence of CSL-GB in the microstructure of grains refined by SPD in copper alloys. LU *et al*. [29] studied the influence of twin boundaries in the UFG of a pure Cu alloy. The authors suggested that when presenting a high density of twin boundaries, the metal will increase mechanical strength without affecting electrical conductivity [29]. Similar results were identified by ZHANG *et al*. [28] regarding the impact of twin boundaries on the strength and electrical conductivity of a bulk nanograined Cu.

A previous article [8] showed the properties evolution of the CuCrZr alloy after being deformed by ECAP and subsequently aged. A three-step rotary swaging was added to improve the mechanical properties further. However, the plastic deformation provided by swaging led to a reduction in the mechanical strength. It is believed that the structure of the grain boundaries, especially the CSL-GB, remained from the previous processes (ECAP and aging) and may partially explain this phenomenon.

Therefore, the main objective of this research is to identify the influence of CSL-GB on the hardness and electrical conductivity of a CuCrZr alloy subject to rotary swaging after having undergone SPD and aging.

2. MATERIALS AND METHODS

A commercial CuCrZr alloy with the following composition in wt%: 0.65 Cr, 0.08 Zr, max. 0.05 Al, max. 0.05 Si, max. 0.05 Fe, max. 0.05 Pb, balance Cu, was used in this research. This was supplied as a round bar of diameter 9.8 mm and length 70 mm.

At first, the specimens were subjected to a solutionizing heat treatment at 1000 °C for 1 h in an argon atmosphere furnace, followed by water quenching [8].

Then, the samples were processed via ECAP at room temperature for up to 10 passes using route Bc, where the sample is rotated by 90° in the same direction between consecutive passes. The ECAP processing was carried out in a circular cross-section die with an internal angle of 120° and an outer curvature arc of 22°. The samples were covered with MoS_2 for lubrication.

After ECAP deformation up to 10 passes, the samples were submitted to an aging heat treatment at 400 °C for 1.5 h with a constant heating rate of 10 °C/mm in an argon atmosphere furnace [8].

The aged ECAP-deformed samples were subsequently processed via rotary swaging at room temperature. The following swaging passes were then performed to achieve the final circular swaged bars with a diameter of 3 mm. Table 1 shows all sample nomenclatures produced.

Mechanical properties were evaluated by the Vickers hardness test with a load of 98 N and an exposure time of 20 s. Electrical conductivity measurements were performed using the four-point technique.

Dislocation density values were determined via X-ray diffraction profile analysis by the Convolutional Multiple Whole Profile software, CMWP, available in http://www.renyi.hu/cmwp site. The diffractograms were

Table 1: Nomenclatures of all produced samples.

CONDITION	NOMENCLATURES
as-received	CR
solutionized	CS
deformed by 10 ECAP pass	C10X
aged	CA
swaged Ø 3.5 mm	CW3.5
swaged Ø 3.2 mm	CW3.2
swaged Ø 2.9 mm	CW2.9

performed using the PANalytical X'PERT PRO MRD diffractometer with Co Kα radiation and operated at 40 KV and 45 mA.

Average grain size, grain size distribution, and grain boundary qualification were performed on the longitudinal sections using a Quanta FEG 250 scanning electron microscope equipped with a Bruker electron backscattering diffraction (EBSD) analyzer and the ESPRIT CrystAlign software. The specimens for EBSD analyses were previously electrochemically polished at room temperature using an electrolyte of HNO3:CH3OH=½:1. The EBSD scan step size was 0.5 µm for the received and solutionized samples and 0.2 µm for other specimens. The average grain size was calculated as a function of the weighted area by ESPRIT CrystAlign software and by MTEX, a Matlab toolbox. In this analysis, we considered grain boundary with misorientation equal to or greater than 15°. The grain size distribution was considered coarse grain for size similar to or greater than 10 µm, medium grain size for the range of 1 µm <d <10 µm and fine grain for measure equal to or less 1 µm. CSL-GBs were obtained with the definition of the Brandon criterion [30].

3. RESULTS AND DISCUSSION

The electrical conductivity analysis and dislocation density of the samples are presented in Figure 1. To facilitate its analysis and discussion, the graph was sectioned into four Regions: A, B, C, and D. Region A shows the dislocation density and electrical conductivity evolutions of received and solutionized samples. Region B presents the behavior of deformed and aged samples, and Regions C and D exhibit the properties of the swaged specimens. The A and B regions have already been presented and discussed in the previous article [8]. The decrease in conductivity in Region A was assigned to precipitate dissolution during the solutionizing process. Meanwhile, in Region B, the sharp decrease in electrical conductivity was due to the increase of dislocation density introduced by the deformation process followed by the substantial increase of electrical conductivity promoted by the aging effect as precipitation of finer Cr- and Zr-rich precipitates.

After aging, the deformation imposed by the three stages of swaging led to a decrease in conductivity from 91.97% IACS (CA) to 87.05% IACS (CW2.9).

As seen in Region C, the lower conductivity is probably related to the evolution of dislocation density, which leaped from 1.022×10^{14} m^{-2} (CA) to 1.714×10^{14} m^{-2} (CW3.2).

Region D presented the same conductivity decrease tendency, although a decrease in dislocation density was also observed (1.219×10^{14} m^{-2}). Hence, the dislocation density is not the primary influencer parameter here. This observed decrease in conductivity can be better understood by analyzing the microstructure and distribution of grain sizes and grain boundary types through the performed steps.

Figure 2 shows the microstructure evolution presenting grain boundary maps, and Figure 3 indicates the percentual variation of CSL-GBs of primary, secondary, and tertiary twins (Σ3, Σ9 e Σ27, respectively) and also random boundaries with electrical conductivity variation superimposed for each condition. It's worth mentioning that the final condition represents the microstructure of the three steps of swaging since the visual aspect was similar.

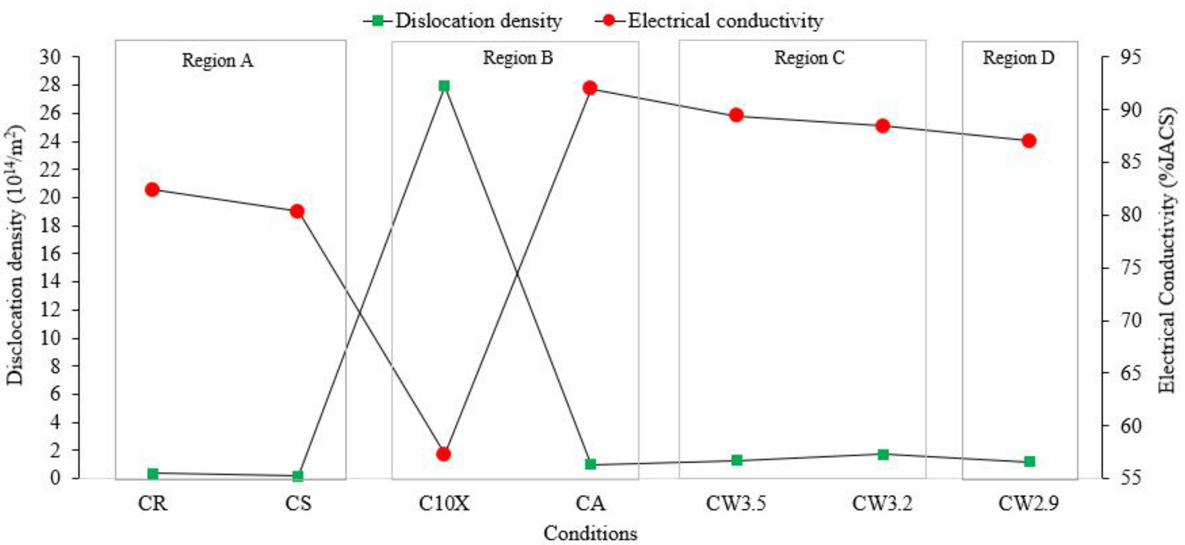

Figure 1: Dislocation density and electrical conductivity evolutions.

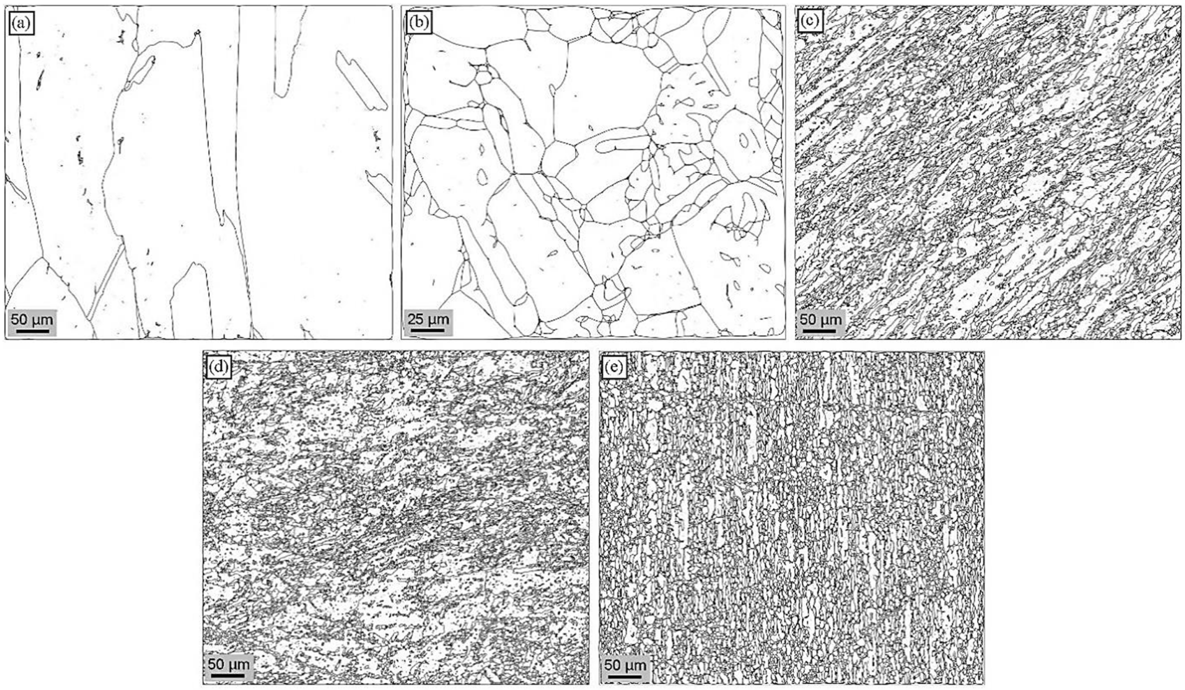

Figure 2: Grain boundary maps obtained by EBSD of (a) CR, (b) CS, (c) C10X, (d) CA, and (e) CW2.9 conditions.

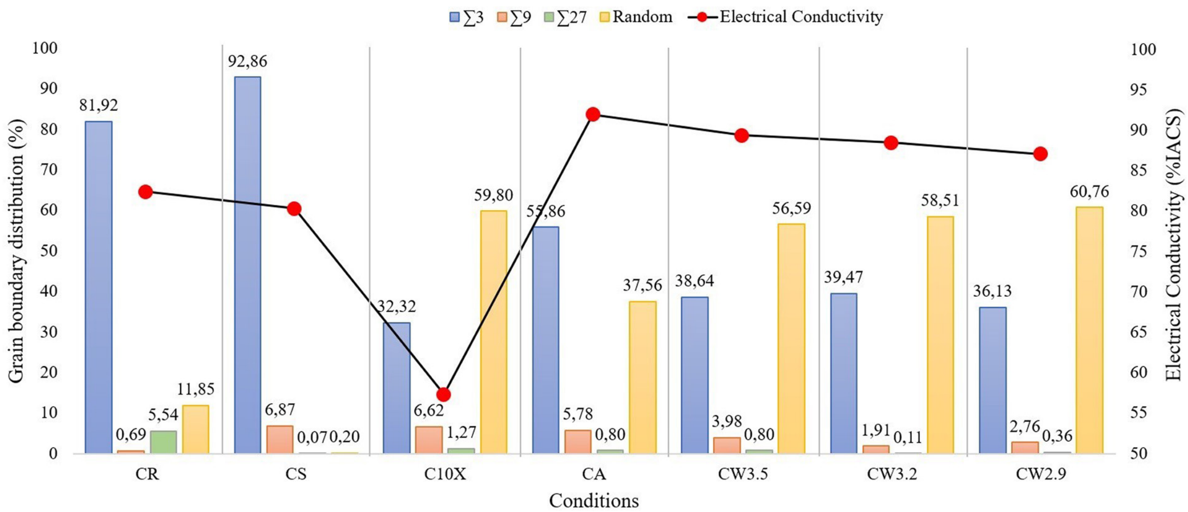

Figure 3: Variation of CSL-GB percentage with electrical conductivity superimposed.

It can be seen that the as-received sample (CR) presented a microstructure with a high superior fraction of ∑3 twin boundaries concerning the other boundary types. These CSL boundaries correspond to annealing twins from the material fabrication [31]. The solutionizing process enhanced the fraction of Σ3 and Σ9 and reduced Σ27 and random boundaries. After the ten passes of ECAP, the microstructure has shown a decrease in low-Σ and an increase in high-Σ and random boundaries as expected [8, 12, 32]. The aging resulted in a rise in the fraction of Σ3 and a decrease of Σ9, Σ27, and random boundaries. As can be observed in Figure 3, there is a decrease of Σ3 boundaries from 39.47% (CW3.2) to 36.13% (CW2.9) and a concomitant increase of Σ9, Σ27, and random grain boundaries. As mentioned, Σ3 has lower resistivity than other CSL-GB and random boundaries [16, 26, 27]. Therefore, the growth of random boundaries and CSL-GB with higher-Σ has possibly enhanced the sample's resistivity, or in other words, it has worsened the conductivity. Furthermore, it is worth mentioning

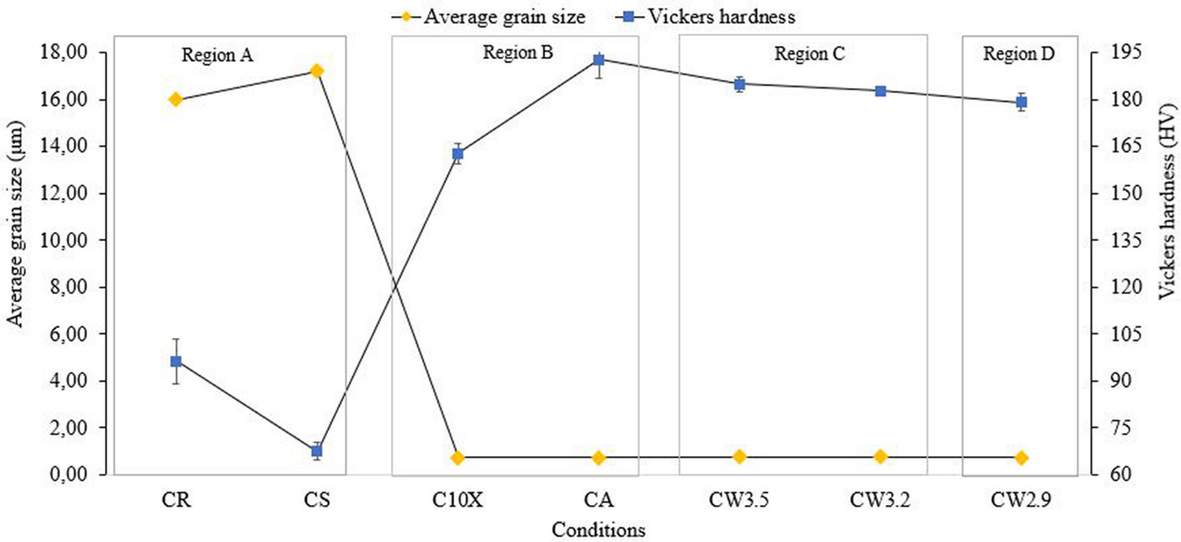

Figure 4: Average grain size and hardness evolutions.

that simultaneously a very light grain refinement (from 0.76 µm (CW3.2) to 0.73 µm (CW2.9)). If the grain is smaller, the total area of grain boundaries per unit volume is higher. Thus, the electronic mobility is reduced since the grain boundaries act as barriers to electron passages [9, 33–36].

As reported by other authors [37–41], the decrease in dislocation density observed in the sample CW2.9 can indicate dynamic recovery (DR). During DR, a portion of the deformation energy is dissipated by means of dislocation annihilation in grain boundary regions [12, 35, 42]. Mobile boundaries are necessary to accommodate such dislocations [12, 37–40, 43]. As reported by other articles, HAGB (especially those with misorientation between 20 and 45°) own higher energy and mobility [44, 45]. On the other hand, CSL-GB present lower energy and mobility [23, 46–48]. This phenomenon can explain the observed in the sample CW2.9, which has shown a decrease in Σ3 and an increase in Σ9, Σ27, and random. The higher number of mobile boundaries (higher Σ and random) may have provided more dislocation annihilation.

Regarding the hardness, a discussion about Regions A and B (Figure 4) has already been presented in a previous article [8]. This property decreased in Region A due to precipitate dissolution during solutionizing. The Region B rise was attributed to the grain refinement provided by the ECAP processing with subsequent precipitation aging.

The swaging after aging was done to strengthen the material by plastic deformation. However, the result was deleterious. As can be seen in Figure 4, the hardness gradually decreased in Regions C and D.

This reduction was explained by the concept of "softening by deformation." With increasing deformation, the microstructure undergoes substantial refinement, finally reaching a steady state of UFG, increasing strength, and reaching a saturation level. However, the unusual behavior of softening by deformation occurs with decreasing strength while the severity of deformation increases. This phenomenon is reported by KAPOOR *et al*. [13] and others [33, 49–52] in UFG obtained by SPD. In their vision, the high amount of randon boundaries can cause grain boundary sliding as a primary or secondary deformation mechanism. In the present case, the HAGB is thought to play an essential role in grain boundary sliding as a secondary deformation mechanism [13].

The smooth decrease in the hardness of sample CW3.5 can be related to the light grain growth observed. As reported, they raised from 0.74 µm (CA) to 0.76 µm (CW3.5).

For samples CW3.2, the hardness decreased by 1.14% concerning the previous value, but the grain size was not changed (0.76 µm). It can be understood by analyzing the volume fraction of grain boundary types in Figure 3. The CSL-GB percentage (%Σ3 + %Σ9 + %Σ27) decreased from 43.42% (CW3.5) to 41.49% (CW3.2) as the expense of increasing in 1.92% of random boundaries. It is well known that CSL-GB is highly resistant to sliding and difficult dislocation movement more efficiently than HAGB [21, 29, 53]. Hence, the reduction of CSL-GB and a concomitant rise in randon boundaries can decrease hardness since dislocations have more freedom to move during plastic deformation [28, 29, 54].

The sample CW2.9 (Region D of Figure 4) presented a slight grain refinement (from 0.76 µm to 0.73 µm) and decay in hardness. The dislocation density decrease can explain such behavior. TERADA *et al*. [47] reported softening in an aluminum alloy processed by ECAP despite reducing grain size. The authors suggested it occurred due to lower dislocation density due to dynamic recovery. Several articles also reported similar assumptions [34, 38, 49, 55]. Furthermore, the Σ3 reductions may have also decreased hardness [28, 30, 56].

Using Figure 3, analyzing the evolution of GB structures in the processes before swaging is also possible. The as-received sample (CR) presented a microstructure with a higher fraction of Σ3 twin boundaries concerning the other types of boundaries. These CSL boundaries correspond to annealing twins from the material fabrication [39]. The solutionizing process enhanced the fraction of Σ3 and Σ9 and reduced Σ27 and random boundaries. After the ten passes of ECAP, the microstructure has shown a decrease in Σ3 and Σ9 and an increase in Σ27 and random grain boundaries as expected [8, 12, 32]. Aging resulted in a rise in a fraction of Σ3 and a reduction of Σ9, Σ27, and random boundaries.

Despite the influence of CSL grain boundaries on the variation of mechanical and electrical properties demonstrated in the present article, some researchers [57, 56] also attribute these modifications to other phenomena like the ideal misorientation and triple junction distribution. However, since the main objective of this research was to identify the influence of CSL-GB on hardness and electrical conductivity, other factors were out of the scope of this study.

4. CONCLUSION

The present paper presents a study about the influence of grain size and types of grain boundaries on the hardness and electrical conductivity of a commercial CuCrZr alloy submitted to SPD, followed by aging and rotary swaging. Based on this, the following conclusions were drawn:

– For the CuCrZr alloy processed by rotary swaging with preexistent UFG, when the dislocation density ceases to be the significant influencer parameter on the electrical conductivity properties, the grain boundary types become more impactful on the change of this property.
– The "softening by deformation" phenomenon was identified throughout the three swaging steps.
– It was realized that reducing CSL-GB and a concomitant rise in randon boundaries can decrease hardness since dislocations have more freedom to move during plastic deformation.
– The dislocation density reduction due to dynamic recovery and the decrease in twin boundaries (Σ3) led to the decline in hardness.

5. ACKNOWLEDGMENTS

The authors thank the Brazilian agencies CNPq and CAPES for their financial support—and the Military Institute of Engineering for assistance and support throughout this research. The authors also acknowledge the Federal University of São Carlos (UFSCar) for the support in the ECAP process, the University of São Paulo (USP) for the assistance in the swaging, and the Estate University of Norte Fluminense (UENF) for the measurements of electrical conductivity.

6. BIBLIOGRAPHY

[1] PURCEK, G., YANAR, H., SHANGINA, D.V., *et al*., "Influence of high pressure torsion-induced grain refinement and subsequent aging on tribological properties of Cu-Cr-Zr alloy", *Journal of Alloys and Compounds*, v. 742, pp. 325–333, 2018. doi: http://doi.org/10.1016/j.jallcom.2018.01.303.

[2] HUMPHREYS, F.J., "Review grain and subgrain characterization by electron backscatter diffraction", *Journal of Materials Science*, v. 36, n. 16, pp. 3833–3854, 2001. doi: http://doi.org/10.1023/A:1017973432592.

[3] KOCICH, R., KUNČICKÁ, L., MACHÁČKOVÁ, A., *et al*., "Improvement of mechanical and electrical properties of rotary swaged Al-Cu clad composites", *Materials & Design*, v. 123, pp. 137–146, 2017. doi: http://doi.org/10.1016/j.matdes.2017.03.048.

[4] CHEN, W., FENG, P., DONG, L., *et al*., "Experimental and theoretical analysis of microstructural evolution and deformation behaviors of CuW composites during equal channel angular pressing", *Materials & Design*, v. 142, pp. 166–176, 2018. doi: http://doi.org/10.1016/j.matdes.2018.01.032.

[5] WANG, B., ZHANG, Y., TIAN, B., *et al*., "Nanoscale precipitates the evolution and strengthening mechanism of the aged Cu-Mg-Fe-Sn-P-Y electrical contact wire", *Journal of Materials Research and Technology*, v. 9, n. 3, pp. 6352–6359, 2020. doi: http://doi.org/10.1016/j.jmrt.2020.03.051.

[6] CAO, X.M., ZHU, Y.B., GUO, F., *et al*., "Study on microstructure and properties of Aged Cu-Ti-Zr-RE alloy", *Advanced Materials Research*, v. 79–82, pp. 1687–1690, 2009. doi: http://doi.org/10.4028/www.scientific.net/AMR.79-82.1687.

[7] ABIB, K., AZZEDDINE, H., TIRSATINE, K., *et al.*, "Thermal stability of Cu-Cr-Zr alloy processed by equal-channel angular pressing", *Materials Characterization*, v. 118, pp. 527–534, 2016. doi: http://doi.org/10.1016/j.matchar.2016.07.006.

[8] SOUSA, T.G., MOURA, I.A.B., GARCIA FILHO, F.D.C., *et al.*, "Combining severe plastic deformation and precipitation to enhance mechanical strength and electrical conductivity of Cu–0.65Cr–0.08Zr alloy", *Journal of Materials Research and Technology*, v. 9, n. 3, pp. 5953–5961, 2020. doi: http://doi.org/10.1016/j.jmrt.2020.03.124.

[9] HUANG, A.H., WANG, Y.F., WANG, M.S., *et al.*, "Optimizing the strength, ductility, and electrical conductivity of a Cu-Cr-Zr alloy by rotary swaging and aging treatment", *Materials Science and Engineering A*, v. 746, pp. 211–216, 2019. doi: http://doi.org/10.1016/j.msea.2019.01.002.

[10] KVAČKAJ, T., BIDULSKY, R., KOVACOVA, A., *et al.*, "Analysis of metallic materials for ITER with the emphasis on copper alloys", *Acta Metallurgica Slovaca*, v. 20, n. 4, pp. 397–404, 2014. doi: http://doi.org/10.12776/ams.v20i4.438.

[11] KAPOOR, G., KVACKAJ, T., HECZEL, A., *et al.*, "The influence of severe plastic deformation and subsequent annealing on the microstructure and hardness of a Cu-Cr-Zr alloy", *Materials*, v. 13, n. 10, pp. 2241, 2020. doi: http://doi.org/10.3390/ma13102241. PubMed PMID: 32414095.

[12] KNAUER, E., FREUDENBERGER, J., MARR, T., *et al.*, "Grain refinement and deformation mechanisms in room temperature severe plastic deformed Mg-AZ31", *Metals*, v. 3, n. 3, pp. 283–297, 2013. doi: http://doi.org/10.3390/met3030283.

[13] KAPOOR, R., SARKAR, A., YOGI, R., *et al.*, "Softening of Al during multi-axial forging in a channel die", *Materials Science and Engineering A*, v. 560, pp. 404–412, 2013. doi: http://doi.org/10.1016/j.msea.2012.09.085.

[14] GLEITER, H., "Nanocrystalline materials", *Progress in Materials Science*, v. 33, n. 4, pp. 223–315, 1989. doi: http://doi.org/10.1016/0079-6425(89)90001-7.

[15] HAMADA, S., KAWAHARA, K., TSUREKAWA, S., *et al.*, "Impact of grain boundary character on electrical property in polycrystalline silicon", *Proceedings of the Materials Research Society*, v. 586, pp. 163–168, 1999. doi: http://doi.org/10.1557/PROC-586-163.

[16] WANG, Z.J., TSUREKAWA, S., IKEDA, K., *et al.*, "Relationship between electrical activity and grain boundary structural configuration in polycrystalline silicon", *Interface Science*, v. 7, n. 2, pp. 197–205, 1999. doi: http://doi.org/10.1023/A:1008796005240.

[17] WINNING, M., "Grain boundary engineering by application of mechanical stresses", *Scripta Materialia*, v. 54, n. 6, pp. 987–992, 2006. doi: http://doi.org/10.1016/j.scriptamat.2005.11.042.

[18] POLYAKOVA, V.V., SEMENOVA, I.P., POLYAKOV, A.V., *et al.*, "Influence of grain boundary misorientations on the mechanical behavior of a near-α Ti-6Al-7Nb alloy processed by ECAP", *Materials Letters*, v. 190, pp. 256–259, 2017. doi: http://doi.org/10.1016/j.matlet.2016.12.083.

[19] SEMENOVA, I., SALIMGAREEVA, G., COSTA, G., *et al.*, "Enhanced strength and ductility of ultrafine-grained Ti processed by severe plastic deformation", *Advanced Engineering Materials*, v. 12, n. 8, pp. 803–807, 2010. doi: http://doi.org/10.1002/adem.201000059.

[20] JIA, H., BJØRGE, R., CAO, L., *et al.*, "Quantifying the grain boundary segregation strengthening induced by post-ECAP aging in an Al-5Cu alloy", *Acta Materialia*, v. 155, pp. 199–213, 2018. doi: http://doi.org/10.1016/j.actamat.2018.05.075.

[21] KOKAWA, H., WATANABE, T., KARASHIMA, S., "Sliding behavior and dislocation structures in aluminum grain boundaries", *Philosophical Magazine. A. Physics of Condensed Matter. Defects and Mechanical Properties*, v. 44, n. 6, pp. 1239–1254, 1981. doi: http://doi.org/10.1080/01418618108235806.

[22] PALUMBO, G., KING, P.J., AUST, K.T., *et al.*, "Grain boundary design and control for intergranular stress-corrosion resistance", *Scripta Metallurgica et Materialia*, v. 25, n. 8, pp. 1775–1780, 1991. doi: http://doi.org/10.1016/0956-716X(91)90303-I.

[23] THAVEEPRUNGSRIPORN, V., WAS, G.S., "The role of coincidence-site-lattice boundaries in creep of Ni-16Cr-9Fe at 360 °C", *Metallurgical and Materials Transactions. A, Physical Metallurgy and Materials Science*, v. 28, n. 10, pp. 2101–2112, 1997. doi: http://doi.org/10.1007/s11661-997-0167-6.

[24] GOODHEW, P.J., "Annealing twin formation by boundary dissociation", *Metal Science*, v. 13, n. 3–4, pp. 108–112, 1979. doi: http://doi.org/10.1179/msc.1979.13.3-4.108.

[25] PRIESTER, L., LARTIGUE, S., "Description and role in high-temperature deformation of grain boundaries in α-alumina ceramics", *Journal of the European Ceramic Society*, v. 8, n. 1, pp. 47–57, 1991. doi: http://doi.org/10.1016/0955-2219(91)90092-E.

[26] TSOUTSOUVA, M.G., VULLUM, P.E., ADAMCZYK, K., *et al*., "Interfacial atomic structure and electrical activity of nano-facetted CSL grain boundaries in high-performance multicrystalline silicon", *Journal of Applied Physics*, v. 127, n. 12, pp. 125109, 2020. doi: http://doi.org/10.1063/1.5130996.

[27] NAKAMICHI, I., "Electrical resistivity and grain boundaries in metals", *Materials Science Forum*, v. 207–209, pp. 47–58, 1996. doi: http://doi.org/10.4028/www.scientific.net/MSF.207-209.47.

[28] ZHANG, Y., LI, Y.S., TAO, N.R., *et al*., "High strength and high electrical conductivity in bulk nanograined Cu embedded with nanoscale twins", *Applied Physics Letters*, v. 91, n. 21, pp. 211901, 2007. doi: http://doi.org/10.1063/1.2816126.

[29] LU, L., SHEN, Y., CHEN, X., *et al*., "Ultrahigh strength and high electrical conductivity in copper", *Science*, v. 304, n. 5669, pp. 422–426, 2004. doi: http://doi.org/10.1126/science.1092905. PubMed PMID: 15031435.

[30] BRANDON, D.G., "The structure of high-angle grain boundaries", *Acta Metallurgica*, v. 14, n. 11, pp. 1479–1484, 1966. doi: http://doi.org/10.1016/0001-6160(66)90168-4.

[31] MISHNEV, R., SHAKHOVA, I., BELYAKOV, A., *et al*., "Deformation microstructures, strengthening mechanisms, and electrical conductivity in a Cu–Cr–Zr alloy", *Materials Science and Engineering A*, v. 629, pp. 29–40, 2015. doi: http://doi.org/10.1016/j.msea.2015.01.065.

[32] STARINK, M.J., "Dislocation versus grain boundary strengthening in SPD processed metals: non-causal relation between grain size and strength of deformed polycrystals", *Materials Science and Engineering A*, v. 705, pp. 42–45, 2017. doi: http://doi.org/10.1016/j.msea.2017.08.069.

[33] SORGER, G.L., OLIVEIRA, J.P., INÁCIO, P.L., *et al*., "Non-destructive microstructural analysis by electrical conductivity: Comparison with hardness measurements in different materials", *Journal of Materials Science and Technology*, v. 35, n. 3, pp. 360–368, 2019. doi: http://doi.org/10.1016/j.jmst.2018.09.047.

[34] MIYAJIMA, Y., KOMATSU, S., MITSUHARA, M., *et al*., "Change in electrical resistivity of commercial purity aluminum severely plastic deformed", *Philosophical Magazine*, v. 90, n. 34, pp. 4475–4488, 2010. doi: http://doi.org/10.1080/14786435.2010.510453.

[35] ORLOVA, T.S., MAVLYUTOV, A.M., BONDARENKO, A.S., *et al*., "Influence of grain boundary state on the electrical resistivity of ultrafine grained aluminum", *Philosophical Magazine*, v. 96, n. 23, pp. 2429–2444, 2016. doi: http://doi.org/10.1080/14786435.2016.1204022.

[36] HUANG, X., HANSEN, N., TSUJI, N., "Hardening by annealing and softening by deformation in nanostructured metals", *Science*, v. 312, n. 5771, pp. 249–251, 2006. doi: http://doi.org/10.1126/science.1124268. PubMed PMID: 16614217.

[37] WARYOBA, D.R., KALU, P.N., CROOKS, R., "Grain-boundary structure of oxygen-free high-conductivity (OFHC) copper subjected to severe plastic deformation and annealing", *Materials Science and Engineering A*, v. 494, n. 1–2, pp. 47–51, 2008. doi: http://doi.org/10.1016/j.msea.2007.09.083.

[38] MISHIN, O.V., GERTSMAN, V.Y., VALIEV, R.Z., *et al*., "Grain boundary distribution and texture in ultrafine-grained copper produced by severe plastic deformation", *Scripta Materialia*, v. 35, n. 7, pp. 873–878, 1996. doi: http://doi.org/10.1016/1359-6462(96)00222-9.

[39] MISHNEV, R., SHAKHOVA, I., BELYAKOV, A., *et al*., "Deformation microstructures, strengthening mechanisms, and electrical conductivity in a Cu–Cr–Zr alloy", *Materials Science and Engineering A*, v. 629, pp. 29–40, 2015. doi: http://doi.org/10.1016/j.msea.2015.01.065.

[40] DALLA TORRE, F., LAPOVOK, R., SANDLIN, J., *et al*., "Microstructures and properties of copper processed by equal channel angular extrusion for 1–16 passes", *Acta Materialia*, v. 52, n. 16, pp. 4819–4832, 2004. doi: http://doi.org/10.1016/j.actamat.2004.06.040.

[41] SOUSA, T.G., SORDI, V.L., BRANDAO, L.P., "Dislocation density and texture in copper deformed by cold rolling and ECAP", *Materials Research*, v. 21, n. 1, e20170515, 2017. doi: http://doi.org/10.1590/1980-5373-mr-2017-0515.

[42] REBHI, A., MAKHLOUF, T., NJAH, N., *et al*., "Characterization of aluminum processed by equal channel angular extrusion: effect of processing route", *Materials Characterization*, v. 60, n. 12, pp. 1489–1495, 2009. doi: http://doi.org/10.1016/j.matchar.2009.08.004.

[43] AL-SAMMAN, T., MOLODOV, K., MOLODOV, D.A., *et al*., "Softening and dynamic recrystallization in magnesium single crystals during-axis compression", *Acta Materialia*, v. 60, n. 2, pp. 537–545, 2012. doi: http://doi.org/10.1016/j.actamat.2011.10.013.

[44] HAYAKAWA, Y., SZPUNAR, J.A., "The role of grain boundary character Distribution in secondary recrystallization of electrical steels", *Acta Materialia*, v. 45, n. 3, pp. 1285–1295, 1997. doi: http://doi.org/10.1016/S1359-6454(96)00251-0.

[45] GOTTSTEIN, G., SHVINDLERMAN, S.L., "On the true dependence of grain boundary migration rate on driving force", *Scripta Metallurgica et Materialia*, v. 27, n. 11, pp. 1521–1526, 1992. doi: http://doi.org/10.1016/0956-716X(92)90138-5.

[46] LIN, P., PALUMBO, G., HARASE, J., *et al*., "Coincidence site lattice (CSL) grain boundaries and goss texture development in Fe-3% Si alloy", *Acta Materialia*, v. 44, n. 12, pp. 4677–4683, 1996. doi: http://doi.org/10.1016/S1359-6454(96)00140-1.

[47] HARASE, J., SHIMIZU, R., DINGLEY, D.J., "Texture evolution in the presence of precipitates in Fe-3% Si alloy", *Acta Metallurgica et Materialia*, v. 39, n. 5, pp. 763–770, 1991. doi: http://doi.org/10.1016/0956-7151(91)90276-7.

[48] ENGLER, O., "On the influence of orientation pinning on growth selection of recrystallization", *Acta Materialia*, v. 46, n. 5, pp. 1555–1568, 1998. doi: http://doi.org/10.1016/S1359-6454(97)00354-6.

[49] TERADA, D., HOUDA, H., TSUJI, N., "Effect of strain on hardening by annealing and softening by deformation phenomena in ultra-fine grained aluminum", *Journal of Materials Science*, v. 43, n. 23-24, pp. 7331–7337, 2008. doi: http://doi.org/10.1007/s10853-008-2809-5.

[50] WANG, Q., GAO, B., WANG, K., *et al*., "Dynamic and static softening mechanisms of commercial-purity Zr during double-stage hot compressive deformation", *Materials Science and Engineering A*, v. 820, pp. 141578, 2021. doi: http://doi.org/10.1016/j.msea.2021.141578.

[51] YUAN, J., GONG, L., ZHANG, W., *et al*., "Work softening behavior of Cu–Cr–Ti–Si alloy during cold deformation", *Journal of Materials Research and Technology*, v. 8, n. 2, pp. 1964–1970, 2019. doi: http://doi.org/10.1016/j.jmrt.2019.01.012.

[52] ZHANG, J., XIA, Y., QUAN, G., *et al*., "Thermal and microstructural softening behaviors during dynamic recrystallization in 3Cr20Ni10W2 alloy", *Journal of Alloys and Compounds*, v. 743, pp. 464–478, 2018. doi: http://doi.org/10.1016/j.jallcom.2018.01.399.

[53] SAHU, S., YADAV, P.C., SHEKHAR, S., "Use of hot rolling for generating low deviation twins and a disconnected random boundary network in Inconel 600 alloys", *Metallurgical and Materials Transactions. A, Physical Metallurgy and Materials Science*, v. 49, n. 2, pp. 628–643, 2018. doi: http://doi.org/10.1007/s11661-017-4431-0.

[54] SINHA, S., KIM, D., FLEURY, E., *et al*., "Effect of grain boundary engineering on the microstructure and mechanical properties of copper containing austenitic stainless steel", *Materials Science and Engineering A*, v. 626, pp. 175–185, 2015. doi: http://doi.org/10.1016/j.msea.2014.11.053.

[55] SANGID, D.S., EZAZ, T., SEHITOGLU, H., *et al*., "Energy of slip transmission and nucleation at grain boundaries", *Acta Materialia*, v. 59, n. 1, pp. 283–296, 2011. doi: http://doi.org/10.1016/j.actamat.2010.09.032.

[56] SAHU, S., PATEL, S.K., SHEKHAR, S., "The effect of grain boundary structure on chromium carbide precipitation in alloy 600", *Materials Chemistry and Physics*, v. 260, pp. 124145, 2021. doi: http://doi.org/10.1016/j.matchemphys.2020.124145.

[57] SAHU, S., SHARMA, N.K., PATEL, S.K., *et al*., "The effect of grain boundary structure on sensitization behavior in a nickel-based superalloy", *Journal of Materials Science*, v. 54, n. 2, pp. 1797–1818, 2019. doi: http://doi.org/10.1007/s10853-018-2919-7.